Mechanical anisotropy of AZ31 magnesium alloy sheet investigated by the acoustic emission technique

P. Dobroň[1]*, J. Bohlen[2], F. Chmelík[1], P. Lukáč[1], D. Letzig[2], K. U. Kainer[2]

[1] *Department of Physics of Materials, Charles University, Ke Karlovu 5, CZ 121 16 Prague 2, Czech Republic*
[2] *GKSS-Forschungszentrum GmbH, Max-Planck-Str. 1, D-21502 Geesthacht, Germany*

Received 6 March 2007, received in revised form 3 April 2007, accepted 3 April 2007

Abstract

The mechanical anisotropy of hot rolled AZ31 magnesium alloy has been investigated by measurements of the acoustic emission (AE). Specimens of different orientations between the tensile axis and the rolling direction were deformed at room temperature and at an initial strain rate of 10^{-3} s^{-1} in order to study the microstructure changes during plastic deformation. It is shown that the mechanical anisotropy is linked with the activity of different slip systems (especially of basal slip) and deformation twinning. The AE parameters are correlated with the stress-strain curves and discussed in terms of possible deformation mechanisms.

K e y w o r d s: acoustic emission, tensile testing, AZ31 magnesium sheet

1. Introduction

Magnesium and its alloys belong to the lightest construction materials and therefore they are prospective for use in many technical applications, especially in the automotive industry, where a weight reduction leads to improving fuel efficiency and car performance. However, the limited number of active dislocation slip systems at room temperature (RT) in hexagonal close-packed (hcp) Mg alloys is responsible for poor strength and formability. Presently, the wrought magnesium alloys offer better mechanical properties in comparison to magnesium cast alloys; nevertheless they also show an anisotropic mechanical behaviour, which is based on the texture of this material and also on large differences in the critical resolved shear stress (CRSS) of various slip systems in the hcp-cell of magnesium. Specifically, there is lack of easy slip systems and the CRSS for different slip systems exhibits a significant dependence on temperature and alloying elements, as reported e.g. in [1–4]. The results [5, 6] demonstrate that the CRSS in the basal plane is much lower than that in the other systems. The texture affects the activity of basal slip and also the activation of hard deformation modes such as non-basal slip and also deformation twinning. Reorientation of basal planes due to twinning in hcp metals affords opportunity for dislocation slip in these planes [7, 8].

The acoustic emission (AE) is defined as transient elastic waves generated by sudden release of energy due to local dynamical changes in the material structure such as dislocation slip and twinning [9]. A direct correlation of AE parameters with the stress-strain curve yields information on the dynamic processes involved in plastic deformation of magnesium and its alloys.

The objective of the present paper is a study of the mechanical anisotropy of hot rolled AZ31 magnesium sheet by the AE technique.

2. Experimental procedure

A commercial AZ31B rolled sheet (Mg + 3 wt.% Al + 1 wt.% Zn) in a strain hardened and stress-relieved condition (H24 in terms of ASTM descriptions) with a thickness of 1.0 mm was used for this study.

The specimens (gauge dimensions 125 mm × 20 mm) were deformed in a universal testing machine Zwick® Z50 in tension at RT and at an initial strain rate of 10^{-3} s^{-1}. Tensile tests were performed in vari-

*Corresponding author: tel.: +420 22191 1611; fax: +420 22191 1490; e-mail address: dobronp@karlov.mff.cuni.cz

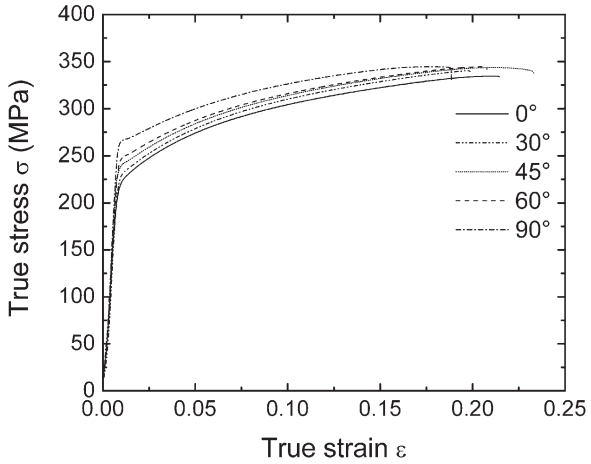

Fig. 1. The true stress *vs.* true strain for hot rolled AZ31 sheet in the H24 condition deformed at angles of 0°, 30°, 45°, 60°, and 90° between the tensile axis and the rolling direction.

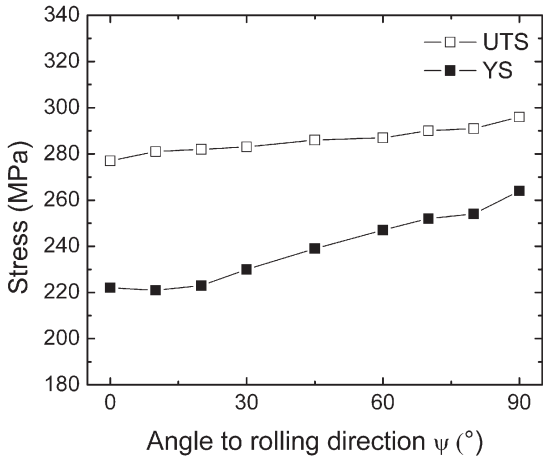

Fig. 2. Mechanical properties as a function of the orientation of the tensile axis to the rolling direction.

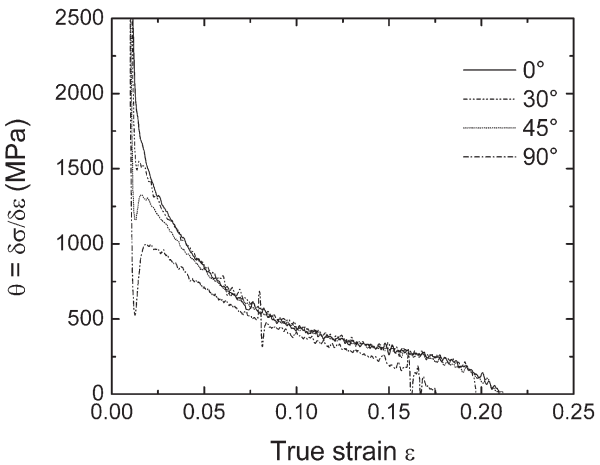

Fig. 3. Work hardening rates as a function of true strain for various orientations of the tensile axis to the rolling direction.

ous orientations ψ of the specimen axis with respect to the rolling direction (RD = 0°).

The computer controlled DAKEL-XEDO-3 AE system was used to monitor AE on the basis of two-threshold-level detection, which yields a comprehensive set of AE parameters involving count rates $\dot{N}_{C_1}$ and $\dot{N}_{C_2}$ (count number per second [10]) at two threshold levels (giving total AE count and burst AE count by proper setting – see below). The burst AE occurs mainly as a consequence of an instable fashion of plastic deformation and, therefore, should respond to twinning. A miniaturized MST8S piezoelectric transducer (diameter 3 mm, almost point AE detection, a flat response in a frequency band from 100 to 600 kHz, sensitivity 55 dB ref. 1 V_{ef}) was attached on the specimen surface with the help of silicon grease and a spring. The total gain was 90 dB. The AE signal sampling rate was 4 MHz, the threshold voltages for the total AE count N_{C_1} and for the burst AE count N_{C_2} were 730 and 1450 mV, respectively. The full scale of the A/D converter was ± 2.4 V.

3. Experimental results

The microstructure of the sheet is shown in [11] illustrating a material containing a large amount of residual stresses and lattice defects. The average grain size of the alloy is 15 μm. Further details can be also found in [11].

The texture [9] is of a strong basal-type with the majority of grains oriented such that the basal planes are nearly parallel to the sheet plane. The basal plane tilt angle is higher with respect to the RD than with respect to the TD. Furthermore, a slight off-basal double peak towards rolling direction indicates a deformation type of texture. The true stress--true strain curves of the samples deformed in tension for angles ψ of 0°, 30°, 45°, 60° and 90° (transversal direction, TD) between the specimen axis and RD are depicted in Fig. 1. Deformation curves are smooth and show pronounced orientation dependence, while conventional tensile yield strength (YS) and ultimate tensile strength (UTS) exhibit the lowest values for the tensile axis parallel to RD and increase with the increasing ψ angle. A yield plateau at the yield point occurred for specimens with orientation angles ψ between 30° and 90°.

Figure 2 shows the dependence of YS and UTS on the orientation angle ψ. It can be seen that with the increasing angle ψ both YS and UTS increase. Furthermore, for ψ higher than 30°, YS increases faster than UTS.

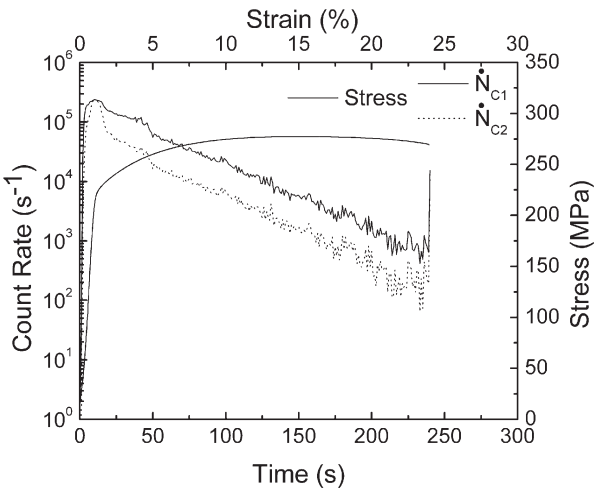

Fig. 4. The correlation between the engineering stress--strain and the AE count rate *vs.* time curves in the rolling direction (0°).

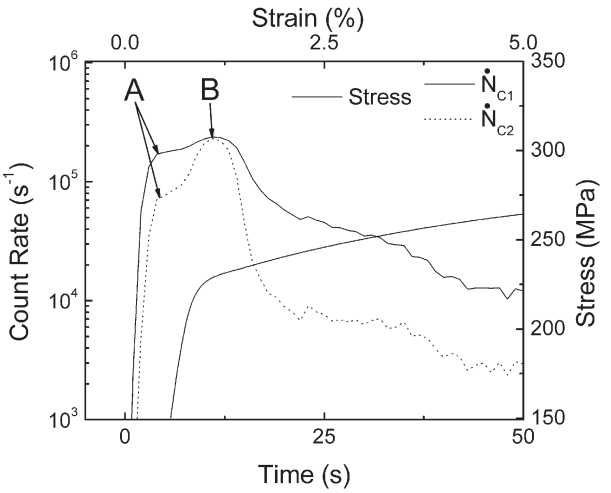

Fig. 6. Detail of two maxima of AE count rate close to the macroscopic yield point for the tensile axis orientation angle of 30° to the rolling direction.

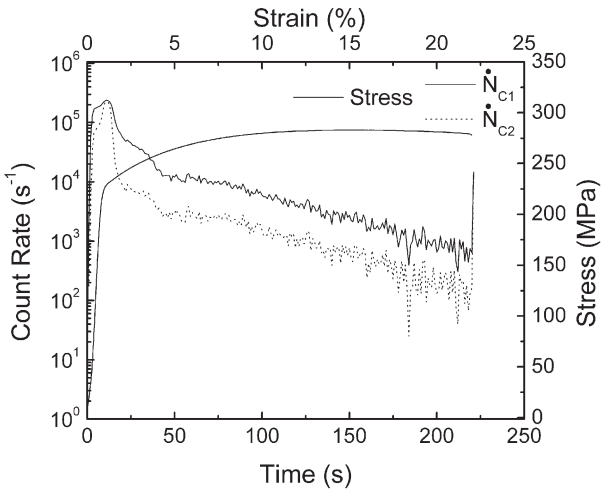

Fig. 5. The correlation between the engineering stress--strain and the AE count rate *vs.* time curves for the tensile axis orientation angle of 30° to the rolling direction.

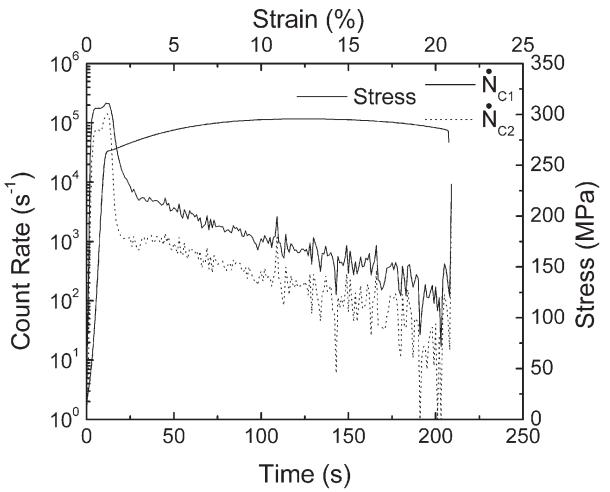

Fig. 7. The correlation between the engineering stress--strain and the AE count rate *vs.* time curves in the transverse direction (90°).

Work hardening rate *vs.* true strain curves for some angles ψ between RD and TD are plotted in Fig. 3. Between $\psi = 30°$ and TD, the curves exhibit a local minimum as a consequence of the occurrence of the yield plateau; the more pronounced is the plateau the more pronounced is the minimum. Note that the work hardening rate decreases with increasing angle ψ.

Figures 4–7 show a correlation between the engineering stress-strain curves and the AE count rate curves for various orientations of the specimen axis to RD. Measurements of the AE activity at two threshold levels (N_{C_1}, N_{C_2}) are helpful to recognize AE signals having a burst character with large amplitude. The AE activity decreases with increasing orientation angle ψ. For all orientations between RD and TD the AE count rate exhibits two maxima closed to the macroscopic yield point (A, B – detailed in Fig. 6), which are followed by a decrease in the count rate lasting until the end of the deformation test. The behaviour of the AE count rates after the second maximum (B) corresponds to the plateau on the deformation curves; the more pronounced is the plateau the lower is the AE activity.

The ratio $\dot{N}_{C_2}/\dot{N}_{C_1}$ *vs.* time depicted in Fig. 8 indicates the relative amount of AE burst signals in the total AE activity during plastic deformation. These

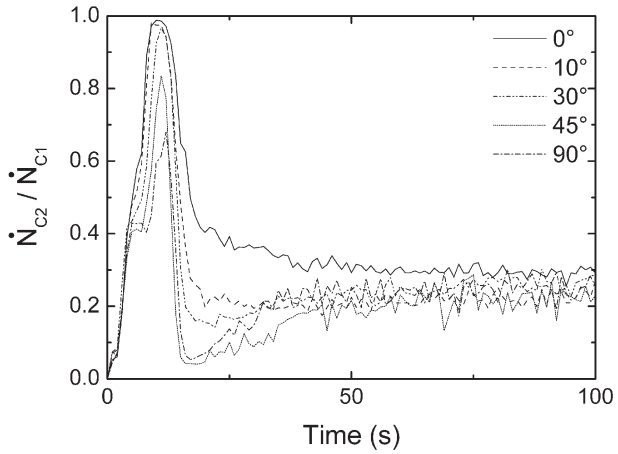

Fig. 8. The ratio of burst emission signals (N_{C_2}) to the total AE activity (N_{C_1}) *vs.* time for some orientations of the tensile axis to the rolling direction.

dependences also exhibit two local peaks within the first 20 seconds of observation.

The first one is more pronounced at higher orientation angles ψ. On the contrary, the second one, which is related to the macroscopic yield point, becomes weaker with increasing orientation angle. The subsequent decay of the ratio $\dot{N}_{C_2}/\dot{N}_{C_1}$ with strain also depends on the orientation angle and for the angles $\psi = 30°$ and more exhibits a local minimum. For later stages of deformation, the curves do not show any significant differences.

4. Discussion

Tensile tests of the AZ31 alloy in the H24 condition performed at RT exhibit the lowest YS in RD, and with increasing orientation angle ψ, the values of YS increase. This result can be explained by different activity of deformation mechanisms owing to the rolling texture of the sheet. Some simulations on the AZ31 alloy in the H24 condition [4, 12] confirm, that besides basal $\langle a\rangle$ slip, prismatic $\langle a\rangle$ slip as well as pyramidal $\langle c + a\rangle$ slip is also activated. In addition, deformation twinning, primarily on $\{10\bar{1}2\}$ planes, may also occur.

A larger tilt angle of basal planes to RD than to the other investigated directions is an ideal condition for the activation of basal $\langle a\rangle$ slip during tensile test due to the lowest CRSS for this slip system. Therefore, more important role of the basal slip during deformation in RD results in lower value of YS in this direction than in other directions (Figs. 1, 2).

According to the geometrical arrangement of basal planes the deformation in TD proceeds by the activation of the prismatic $\langle a\rangle$ slip and later also of the pyramidal $\langle c + a\rangle$ slip. The earlier activation of the prismatic $\langle a\rangle$ slip in spite of its similar CRSS by comparison to the pyramidal one at RT can be explained by the fact that the $\langle c + a\rangle$ dislocations tend to dissociate to the $\langle a\rangle$ and $\langle c\rangle$ dislocations [13–15]. Thus, more rapid strain hardening observed from the angle $\psi = 30°$ up to 90° (Fig. 2) can be explained by the non-basal slip systems activity.

The tensile strain is represented by the width and the thickness strain. The width strain is produced by the prismatic $\langle a\rangle$ slip and the thickness strain is produced by the basal $\langle a\rangle$ slip, the pyramidal $\langle c + a\rangle$ slip and also by twinning. The Lankford r-value is a ratio of the width strain to the thickness strain in a deformed sheet. Kaiser et al. [16] reported that the Lankford r-value in the AZ31 sheet increases roughly from 1.0 in RD to 3.5 in TD, which indicates that the width strain is larger than the thickness strain if the orientation angle ψ increases. From these results we can deduce that the activity of twinning decreases with increasing orientation angle ψ.

The plateau on the deformation curves is likely due to the formation of Lüders bands which are formed when a number of dislocations move one after another in a chain reaction known as the cataclysmic release of dislocations and it is evident that their formation is associated with a significant slip.

Hardening caused by dislocation storage and softening due to recovery processes can also be seen in Fig. 3. For ψ higher than 30° the work hardening rates exhibit local peaks followed by a drop, which can be caused by a higher activity of non-basal slip systems.

The AE peak related to the macroscopic yield point is explained by a massive dislocation multiplication and twinning, which are excellent sources of AE [17]. The following decrease in the AE count rates can be assumed as a consequence of strain hardening. Increasing density of forest dislocations due to interactions between basal $\langle a\rangle$ and pyramidal $\langle c + a\rangle$ dislocations reduces the flight distance of mobile dislocations. A decrease in the free path of moving dislocations leads to the reduction of the AE activity. The slowest decay in the AE count rate is found in RD, with increasing ψ it becomes faster. This can be understood by taking into account a more important role of twinning in RD than in other directions.

The first maximum depicted in Fig. 8 can indicate the activation of primary $\{10\bar{1}2\}$ $\langle 10\bar{1}\bar{1}\rangle$ twins because this twinning mode has the lowest shear stress and involves simple shuffles in the shear plane [18]. Consecutive glide in the reoriented grains and probably also the activation of twins oriented differently to the primary twins (such as in $\{10\bar{1}1\}$ $\langle 10\bar{1}2\rangle$ system, observed in [19]) contributes to strain hardening and reduces the amount of high amplitude AE signals. Since twinning (unlike dislocation glide) will generate AE mainly of the burst type character [17], it may be supposed that the role of twinning will be most

important in RD where the ratio of burst AE to the total AE shows the highest value. The ratio $\dot{N}_{C_2}/\dot{N}_{C_1}$ decreases with increasing orientation angle ψ what indicates increasing role of non-basal slip systems during deformation. Obtained results also correspond to results of Lankford r-value for the AZ31 sheet [16].

Such behaviour is also demonstrated by the orientation dependence of the second peak. This peak becomes less pronounced with increasing angle ψ, which gives hint on a lower activity of twins at the beginning of the plastic deformation. The following decrease of the AE activity can also be caused by the interaction between slip dislocations and deformation twins (hardening by twin boundaries), which is in accordance with the work hardening rates shown in Fig. 3.

5. Conclusions

The hot rolled AZ31 sheets in the H24 condition with various orientations of the specimen axis to the rolling direction were tested in tension at room temperature with concurrent acoustic emission (AE) measurements. The AE count rates showed two peaks close to the macroscopic yield point followed by a subsequent decrease in the AE activity. The results can be explained by the sample-orientation-dependent activation of non-basal slip systems and deformation twinning during plastic deformation. The observed effect of the specimen axis orientation to the rolling direction (mechanical anisotropy) demonstrates the importance of the activation of primary $\{10\bar{1}2\}\langle 10\bar{1}\bar{1}\rangle$ twinning and, consequently, also differently oriented secondary twins at the beginning of plastic deformation.

Acknowledgements

We would like to dedicate this paper to Prof. RNDr. Zuzanka Trojanová, DrSc. on the occasion of her 65th birthday. This work received a support from the Research Project 1M 2560471601 Eco-centre for Applied Research of Non-ferrous Metals which is financed by the Ministry of Education, Youth and Sports of the Czech Republic. Additional support was also provided by the Grant Agency of the Czech Republic under Grant No. 103/06/0708.

References

[1] ANDO, S.—TONDA, H.: Mater. Sci. Forum, *43*, 2000, p. 350.
[2] STAROSELSKY, A.—ANAND, L.: Int. J. Plast., *19*, 2003, p. 1843.
[3] TROJANOVÁ, Z.—GÄRTNEROVÁ, V.—PADALKA, O.: Kovove Mater., *42*, 2004, p. 206.
[4] MÁTHIS, K.—TROJANOVÁ, Z.: Kovove Mater., *43*, 2005, p. 238.
[5] AGNEW, S. R.—TOMÉ, C. N.—BROWN, D. W.—HOLDEN, T. M.—VOGEL, S. C: Scripta Mater., *48*, 2003, p. 1003.
[6] KLEINER, S.—UGGOWITZER, P. J.: Mater. Sci. Eng. A, *379*, 2004, p. 258.
[7] ZHANG, P.—WATZINGER, B.—KONG, P. Q.—BLUM, W.: Key Eng. Mater., *171–174*, 2000, p. 609.
[8] MÁTHIS, K.—MUSSI, A.—TROJANOVÁ, Z.—LUKÁČ, P.—RAUCH, E: Kovove Mater., *41*, 2003, p. 293.
[9] HEIPLE, C. R.—CARPENTER, S. H.: J. Acoustic Emission, *6*, 1987, p. 177.
[10] Standard Practice for Acoustic Emission Examination of Fiberglass Reinforced Plastic Resin, ASTM E 1067-85. Tank/Vessels, 1985.
[11] BOHLEN, J.—CHMELÍK, F.—DOBROŇ, P.—LETZIG, D.—LUKÁČ, P.—KAINER, K. U.: J. Alloys Compd., *378*, 2004, p. 214.
[12] AGNEW, S. R.: In: Magnesium Technology 2002. Ed.: Kaplan, H. I. Columbus, Ohio, The Minerals, Metals & Materials Soc. TMS 2002, p. 169.
[13] OBARA, T.—YOSHINAGA, H.—MOROZUMI, S.: Acta Metall., *21*, 1973, p. 845.
[14] BOHLEN, J.—CHMELÍK, F.—KAISER, F.—LETZIG, D.—LUKÁČ, P.—KAINER, K. U.: Kovove Mater., *42*, 2004, p. 165.
[15] JÄGER, A.—LUKÁČ, P.—GÄRTNEROVÁ, V.: Kovove Mater., *40*, 2002, p. 291.
[16] KAISER, F.—LETZIG, D.—BOHLEN, J.—STYCZYNSKI, A.—HARTIG, C.—KAINER, K. U.: Mater. Sci. Forum, *419–422*, 2003, p. 315.
[17] FRIESEL, M.—CARPENTER, S. H.: J. Acoustic Emission, *3*, 1984, p. 11.
[18] LAY, S. —NOUET, G.: Philos. Mag. A, 70, 1994, p. 261.
[19] MÁTHIS, K.—CHMELÍK, F.—JANEČEK, M.—HADZIMA, B.—TROJANOVÁ, Z.—LUKÁČ, P.: Acta Mater., *54*, 2006, p. 5361.